Letter to the Editor

Biphasic squamoid alveolar renal cell carcinoma: description of a rare case and a literature analysis

Yang Zhang[1]^, Yuyun Xu[1], Taihen Yu[1], Junfa Chen[1], Ming Zhao[2], Chunmiao Lin[1]

[1]Cancer Center, Department of Radiology, Zhejiang Provincial People's Hospital, Affiliated People's Hospital, Hangzhou Medical College, Hangzhou, China; [2]Cancer Center, Department of Pathology, Zhejiang Provincial People's Hospital, Affiliated People's Hospital, Hangzhou Medical College, Hangzhou, China

Correspondence to: Chunmiao Lin, MD. Cancer Center, Department of Radiology, Zhejiang Provincial People's Hospital, Affiliated People's Hospital, Hangzhou Medical College, Hangzhou 310014, China. Email: lcmdb@126.com; Ming Zhao, MD. Cancer Center, Department of Pathology, Zhejiang Provincial People's Hospital, Affiliated People's Hospital, Hangzhou Medical College, Hangzhou 310014, China. Email: zhaomingpathol@163.com.

Submitted Dec 23, 2021. Accepted for publication Apr 12, 2022.
doi: 10.21037/qims-21-1230
View this article at: https://dx.doi.org/10.21037/qims-21-1230

Introduction

Biphasic squamoid alveolar renal cell carcinoma (BSARCC) is a comparatively new concept that was first reported as biphasic alveolosquamoid renal carcinoma in 2012 (1). It was described as a neoplastic feature consisting of 2 unusual nested morphologies with unique cell types.

Thus far, the 2 largest groups of case studies on BSARCC consist of 21 cases reported by Hes *et al.* (2) and 28 cases reported by Trpkov *et al.* (3); however, these reports are limited to pathological studies. Both research groups have asserted that BSARCC consists of 2 distinct cell populations with varying proportions. The first is a population of small cells with sparse cytoplasm and round and slightly extended nuclei that resemble lymphocytes and are arranged in alveolar-like structures, similar to dilated tubules, microcapsules, or glomerular balloon structures. The second is a population of large eosinophilic squamoid cells that form nests in the alveolar-like structures with clustered, micropapillary, or solid clusters in the center of the acinus; and an abundant and eosinophilic cytoplasm, large nuclei, and prominent nucleoli similar to squamous cells, but no obvious intercellular bridges or keratinized beads. Both populations express cytokeratin 7 (CK7), alpha-methylacyl-CoA racemase (AMACR), and vimentin. Interestingly, the most significant immunohistochemical feature of BSARCC is that the expression of cyclin D1 is limited to squamous cells.

Although histological manifestations of this new type of neoplastic feature have been described, few reports have been published on the imaging manifestations of BSARCC. Thus, we report a case of BSARCC with abundant imaging findings that was diagnosed histologically as typical BSARCC.

Case report

All procedures performed in this study were in accordance with the ethical standards of the institutional and/or national research committee(s) and with the Helsinki Declaration (as revised in 2013). Written informed consent was obtained from the patient or legal guardian for publication of this case report and accompanying images. A copy of the written consent is available for review by the editorial office of this journal.

A 39-year-old male with a renal tumor discovered during a health screening by abdominal ultrasound was referred to Zhejiang Provincial People's Hospital, Affiliated People's Hospital for further evaluation. Ultrasound showed a hypoechoic nodule approximately 2.8 cm × 1.8 cm in size with a clear boundary in the right kidney (*Figure 1*). All

^ ORCID: 0000-0001-7276-0488.

tumor markers and test indicators were negative.

Computed tomography (CT) was performed, revealing a 3-cm mass in the mid-portion of the right kidney (*Figure 2*) that was isodense on the unenhanced CT image and slightly enhanced with a clear edge on the enhanced scan. Enhanced magnetic resonance imaging (MRI) was subsequently performed. The lesion was primarily located in the renal medulla and partially protruded into the renal pelvis. The lesion was isointense on T_1-weighted imaging and hypointense on T_2-weighted imaging (T_2WI), had a higher signal on diffusion-weighted imaging, and exhibited mild enhancement in the corticomedullary phase and persistent mild enhancement in the nephrographic phase (*Figure 3*); the apparent diffusion coefficient (ADC) of the lesion was 0.883×10^{-3} mm^2/s. The patient then underwent whole-body ^{18}F-fluorodeoxyglucose (FDG) positron emission tomography (PET)/CT, which confirmed increased glucose metabolism in the right kidney [maximum standardized uptake value (SUVmax) 3.8; *Figure 4*].

Figure 1 B-mode ultrasound showing a 2.8 cm (1: long axis) × 1.8 cm (2: short axis) hypoechoic mass located in the mid-lateral portion of the right kidney in a 39-year-old-man with clear BSARCC. BSARCC, biphasic squamoid alveolar renal cell carcinoma.

After multidisciplinary evaluation, the mass was classified as indeterminate but was considered most consistent with papillary renal cell carcinoma (PRCC). Partial nephrectomy of the right kidney was performed. Pathology confirmed the characteristic histological features of renal cell carcinoma but could not be specifically classified. Samples were also subjected to immunohistochemistry and fluorescent in situ hybridization (FISH).

All slides were reviewed by 3 pathologists, who examined 4-μm hematoxylin- and eosin-stained tissue sections after they had been fixed using 4% formaldehyde and embedded in paraffin according to standard protocols. The following pathological features were determined: (I) the tumor had a little renal tissue, was 3 cm × 3.5 cm × 3 cm in size, had a clear boundary, and had a grey-yellow solid section. (II) The tumor was clearly demarcated from the surrounding renal tissue, and the capsule could not be seen microscopically. (III) The tumor tissue was alveolar and papillary, with a large number of foamy tissue cells in the interstitium. (IV) The tumor was composed of 2 groups of cells: the first group, accounting for approximately 85% of cells, consisted of small tumor cells with a sparse cytoplasm that were basophilic and arranged in multiple layers with small and consistent nuclei, deep chromatin, and nonobvious nucleoli; the second group, accounting for approximately 15% of cells, consisted of larger tumor cells that were polygonal, rich, and eosinophilic, with large nuclei, vacuolated chromatin, and obvious nucleoli. (V) The 2 groups of tumor cells transited and intermingled with one another (*Figure 5*). (VI) In the mixed area, the small cells in tubules or acini

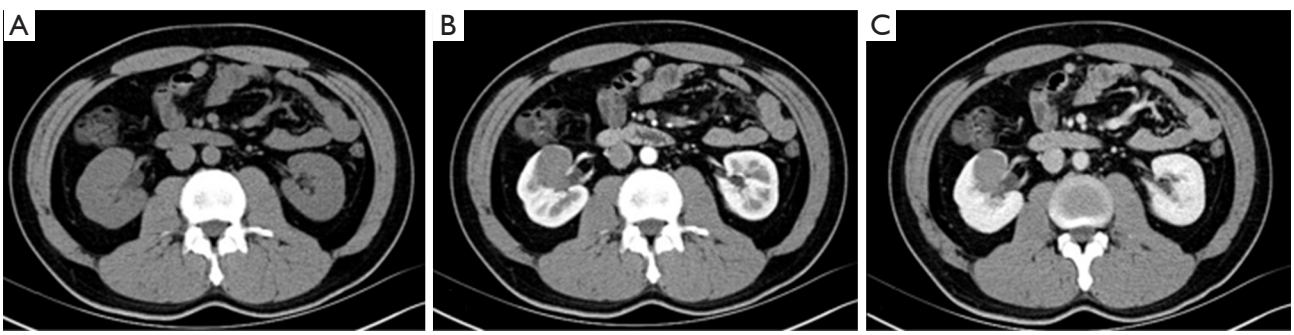

Figure 2 CT of the patient with biphasic squamous alveolar renal cell carcinoma. (A) Abdominal unenhanced CT image showing a round, well-defined isodense, 3-cm nodule in the medulla of the right kidney. (B) The tumor is enhanced slightly and homogeneously during the corticomedullary phase without necrotic or cystic areas in the lesion. (C) The tumor continues to be enhanced homogeneously during the nephrographic phase. CT, computed tomography.

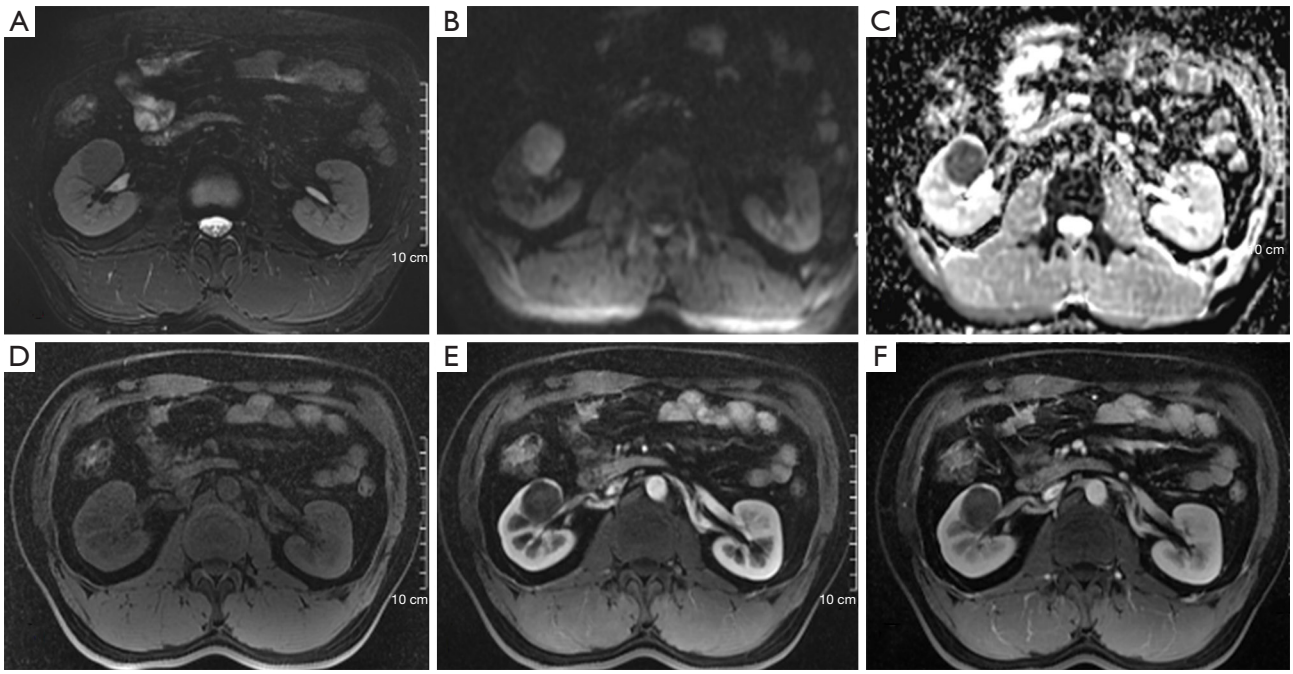

Figure 3 Magnetic resonance images from the patient. (A) Axial fat-suppressed T_2WI showing a homogeneous and notably hypointense 3.5 cm × 3.0 cm mass in the mid-portion of the right kidney. (B) Diffusion-weighted imaging (b =1,000 s/mm^2) showing a homogeneous high signal. (C) ADC imaging showing a homogeneous low signal. (D) Axial fat-suppressed T_1-weighted imaging showing a small, round, isosignal external mass. (E) Corticomedullary phase imaging showing mild homogeneous enhancement inside the mass. (F) Nephrographic phase imaging showing slightly gradual enhancement. T_2WI, T_2-weighted imaging; ADC, apparent diffusion coefficient.

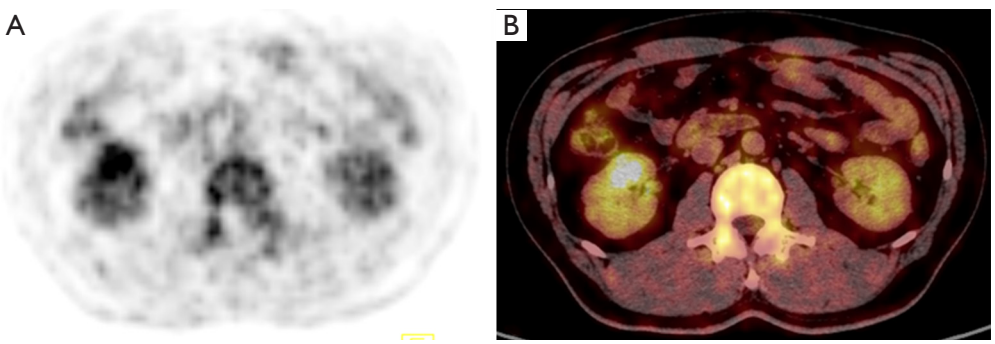

Figure 4 (A) ^{18}F-FDG PET/CT image from the patient showing BSARCC positive for ^{18}F-FDG. (B) Focal FDG radioactivity concentration in the right renal lesion with a SUVmax of 3.8; the SUVmax of the normal renal tissue around the lesion was 1.8. FDG, fluorodeoxyglucose; PET, positron emission tomography; CT, computed tomography; BSARCC, biphasic squamoid alveolar renal cell carcinoma; SUVmax, maximum standardized uptake value.

grew around the larger tumor cells (*Figure 5C*). (VII) No vascular infiltration or extrarenal proliferation was present, and the renal parenchyma margin was negative.

The 4-μm tissue slices obtained as described above were subjected to immunohistochemical staining using a Ventana Benchmark autostainer (Ventana Medical Systems, Tucson, AZ, USA). Immunohistochemical staining showed that paired-box gene 8 (PAX8), CK7, and AMACR were diffusely expressed (>50%) in both groups of tumor cells; the larger cells also expressed vimentin and cyclin D1, but

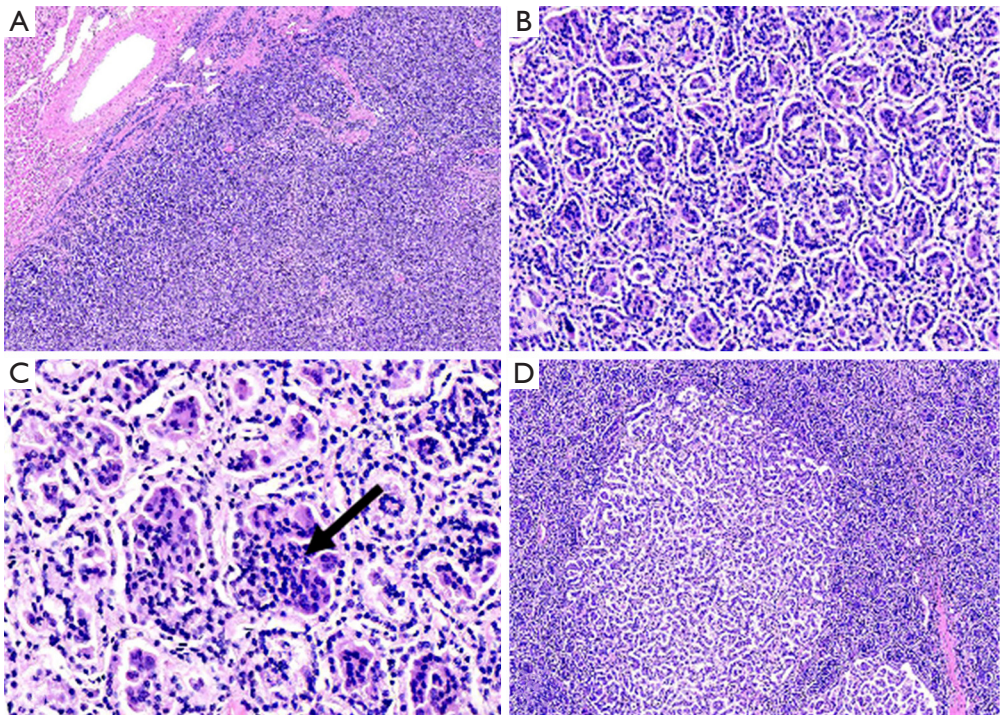

Figure 5 Main pathological features of the BSARCC. (A) The tumors showed solid and clear boundaries without a capsule (H&E) (original magnification ×100). (B) Formation of alveolar or glomeruloid structures by biphasic cells (H&E) (original magnification ×200). (C) Smaller cells are located at the periphery of the acinus with less cytoplasm and a lower nuclear grade; larger cells are located in the center of the acinus with an abundance of eosinophilic cytoplasm and a higher nuclear grade. Emperipolesis (engulfment of hematopoietic cells or parts of cells) can be seen in most tumors with this pattern (H&E) (arrow; original magnification ×400). (D) Transition of the alveolar structure to a typical PRCC can be seen in the focal area (H&E) (original magnification ×100). BSARCC, biphasic squamoid alveolar renal cell carcinoma; H&E, haematoxylin and eosin; PRCC, papillary renal cell carcinoma.

the smaller cells were uniformly negative to these markers. Ki67 primarily labeled the large cells (proliferation index of approximately 10%) but also labeled the small cells (proliferation index of approximately 1%). Neither group of cells expressed CD117, Wilms' tumor 1 (WT1), CD10, or carbonic anhydrase IX (CAIX; *Figure 6*). Cyclin D1 was expressed in the nuclei of the larger but not small tumor cells (*Figure 7*). Centromere 7 and 17 enumeration using FISH was performed (*Figure 8*). Chromosome 7 trisomy was found (20%) in both the small and large cells at the center of the alveolar-like structures, co-occurring with trisomy 17 (24%). There was also accompanying Y-chromosome loss.

After surgery, the patient recovered well, with no tumor recurrence or metastasis observed over a 20-month follow-up.

Discussion

This case report of BSARCC provides the most complete clinical, radiological, and pathological data available in the current literature, and is thus of considerable significance for image collection in future cases.

There is a view that BSARCC is a morphological variant of PRCC and is more closely related to type 1 PRCC (2,3). Another view holds that since the publication of the fourth edition of the World Health Organization (WHO) classification of Tumours of the Urinary System and Male Genital Organs in 2016, a number of additional renal cell carcinoma tumor types have been described and, of these, BSARCC is likely to be included in the next iteration of the WHO classification of renal tumors as a novel tumor type (4). At present, BSARCC is not included in the 2016 WHO Classification of Urogenital Tumors (5,6). Regardless of how BSARCC is eventually classified, the standard of care remains surgical resection with either partial or total nephrectomy.

There have been a few reports published concerning

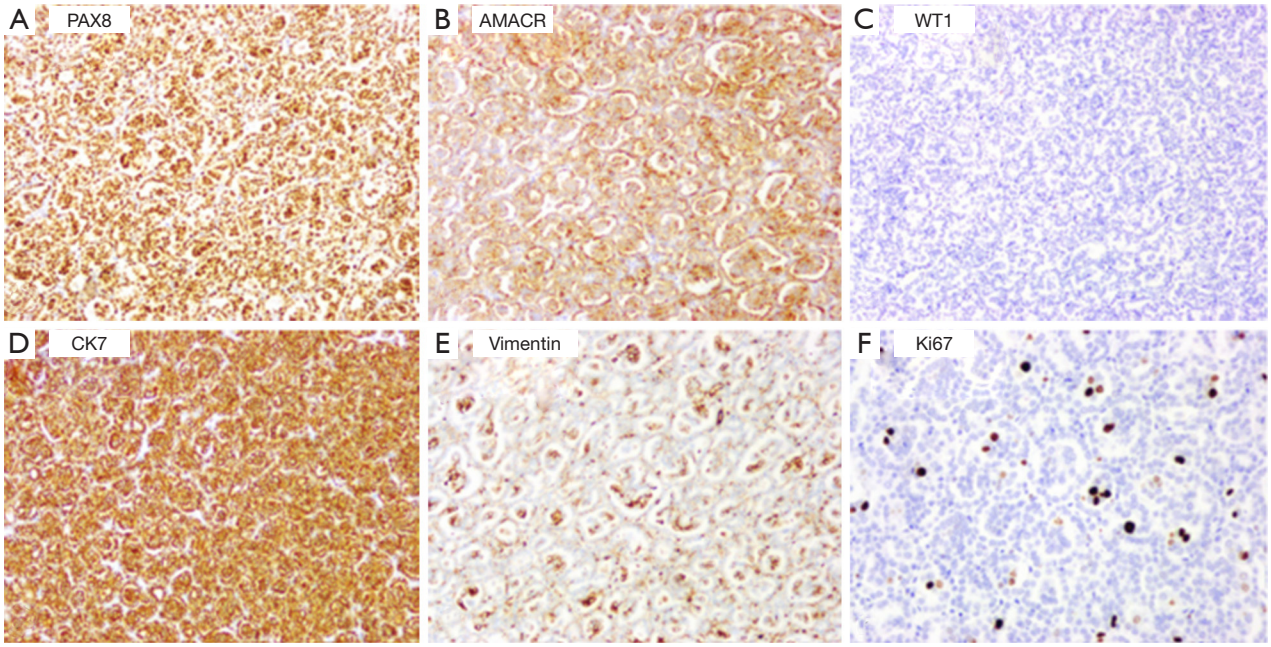

Figure 6 Immunohistochemical evaluation. BSARCC exhibiting (A) strong diffuse cytoplasmic PAX8 staining with peripheral cell accentuation, (B) diffuse cytoplasmic AMACR expression, (C) negative staining for WT1, (D) diffuse cytoplasmic CK7 expression, (E) vimentin-positive staining only in the nuclei of larger cells, with the smaller cells being uniformly negative, and (F) proliferating antigen Ki67 labeling primarily of the population of larger cells (original magnification ×100). BSARCC, biphasic squamoid alveolar renal cell carcinoma; PAX8, paired-box gene 8; AMACR, alpha-methylacyl-CoA racemase; WT1, Wilms' tumor 1; CK7, cytokeratin 7.

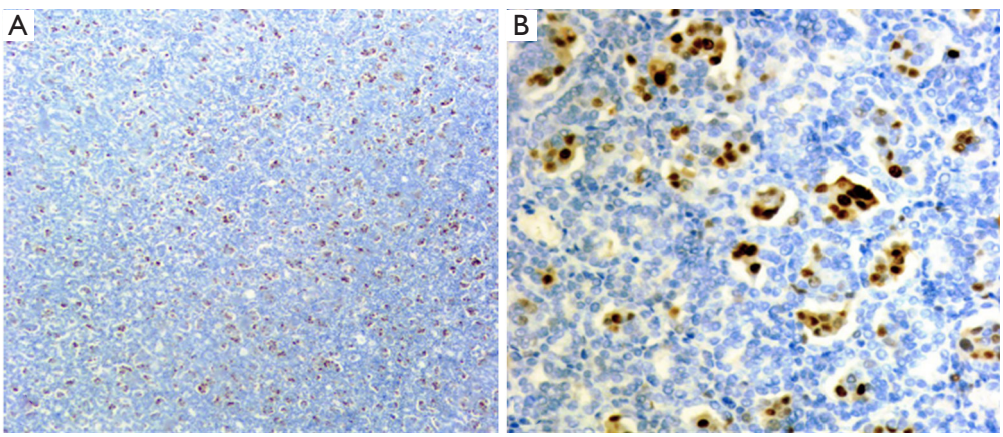

Figure 7 Immunohistochemical evaluation. Only the large squamous cells appear positive for cyclin D1, with the smaller cells being uniformly negative. (A) Original magnification ×40; (B) original magnification ×200.

BSARCC (1-3,7-11). BSARCC appears to occur slightly more frequently in males, with a male-to-female ratio of approximately 1.5:1.0, and has an age of onset ranging from 9 to 86 years (*Table 1*). Two cases have occurred in transplanted kidneys (7) (*Table 1*). Hereditary BSARCC has been described, including 1 patient with Birt-Hogg-Dubé (BHD) syndrome (3) and 1 patient whose condition was associated with hereditary PRCC (9). Approximately one-third of BSARCC cases are multifocal with other types of renal tumors (including PRCC, clear cell renal

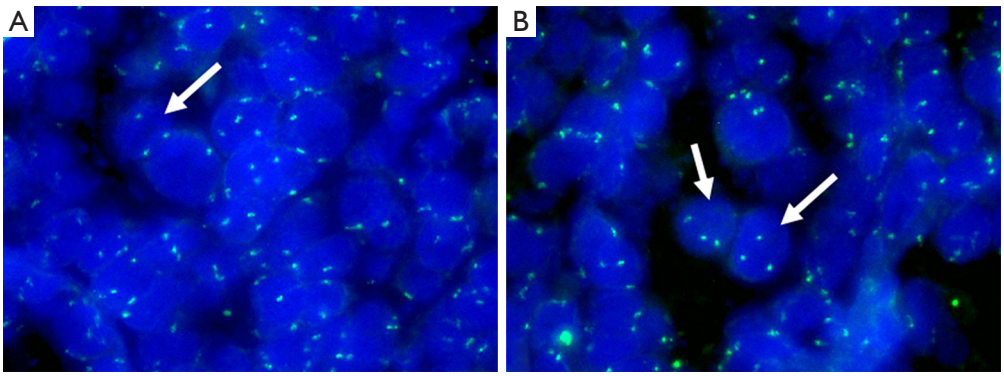

Figure 8 Copy number analysis of (A) centromeres 7 and (B) 17 by FISH. FISH with chromosome 7 and 17 centromeric probes showed chromosome 7 and 17 trisomy (arrows) in approximately 20% and 24% of cells, respectively (original magnification ×1,000). FISH, fluorescent in situ hybridization.

Table 1 Summary of previous reports of BSARCC

Reference	Year	Cases, n	Age (years)	Males, n	History	Location	Size (cm)	Lesion	Highlight
(1)	2012	2	68, 54	1	Incidental carcinoma	Right	3.7, 3	Unifocal	Reported BSARCC for the first time
(2)	2016	21	53–79	11	Unknown	Unknown	1.5–16	Unifocal	Revisited and fully characterized BSARCC
(7)	2016	2	9, 63	1	Kidney allografts	Unknown	2.3, 4.1	Unifocal	Reported BSARCC in allograft kidneys
(8)	2016	1	68	1	Hematuria	Right	1–3	Multifocal	First reported BSARCC case with multifocal lesion
(9)	2017	2	44, 52	1	Nephrectomy	Bilateral	0.1–4	Multifocal	First reported BSARCC case occurring in a familial context associated with *MET* mutation
(3)	2018	28	39–86	18	Unknown	16 left	0.9–6.5	8 multifocal	Confirmed many findings from previous study
(10)	2019	3	36–56	3	Incidental carcinoma	2 left	1–8	Unifocal	BSARCC cases exhibited indolent clinical course, and larger cells expressed cyclin D1 and CD57
(11)	2021	17	26–84	10	Unknown	12 left	1.5–15	3 multifocal	Suggested that *MET* represented a major oncogenic driver gene in BSARCC

BSARCC, biphasic squamoid alveolar renal cell carcinoma.

cell carcinoma, and BHD-related hybrid oncocytic/chromophobe tumor) (3), with a diameter of 0.9–16 cm. However, previous studies have only reported on the pathology of BSARCC and have not provided data on imaging features.

In this case, certain imaging features were observed. The mass involved the medulla and had a clear boundary, whereas PRCC often involves the cortex. After the injection of contrast medium, the tumor appeared as well-defined, homogeneous, and hypovascular masses on CT and MRI. It had a hypointense T_2WI signal and marked hypo-enhancement on all phases of dynamic contrast-enhanced MRI. These imaging findings are similar to those of PRCC (12-14), which may suggest that BSARCC results from a morphological change to PRCC. SUVmax has been evaluated by ^{18}F-FDG PET/CT to predict the survival rate of patients with BSARCC (15). In the present case, SUVmax was approximately 3.8 (i.e., <8), indicating a good prognosis. Indeed, the patient recovered well after surgery, with no tumor recurrence or metastasis during the

20-month follow-up.

Microscopically, BSARCC is characteristically composed of clusters of 2 types of tumor cells with varying proportions. It is generally believed that the proportion of large cells is correlated with survival (16). In this case, the large tumor cells accounted for approximately 15% of tumor cells, and this may predict a better outcome. Meanwhile, the tumor showed the typical biphasic cell composition of BSARCC, with a solid acinar, tubular, and papillary arrangement. The 2 groups of cells fused, transited, and mixed with one other, with sheets of foam cells accumulating in the interstitium.

Evaluating the immunoexpression of these tumors can be helpful diagnostically because they show diffuse positive staining for pan-cytokeratin (cytokeratin AE1/AE3), CK7, racemase, PAX8, epithelial membrane antigen, vimentin, and cyclin D1. Cyclin D1 immunostaining is specific for this tumor, and cyclin D1 was expressed only in the larger cells, which represents a unique and previously not recognized pattern of immunohistochemical staining (2,3,8).

Chromosomal analysis by FISH identified gains of chromosomes 7 and 17 in all 16 BSARCC cases tested (2,3,10), with 80% (4/5) of tumors that developed in male patients having Y-chromosome deletion (2), which is a similar molecular genetic characteristic as that seen in PRCC. Therefore, the histological, immunophenotypic, and molecular genetic characteristics may support BSARCC as a special histological type of PRCC (2,3,9). In this case, the tumor showed immunophenotypic characteristics consistent with those described above for BSARCC, especially diffuse strong cyclin D1 expression in the large tumor cells, trisomy 7 and 17 positivity, and Y-chromosome negativity. Denize *et al*. (11) reported that the proto-oncogene MET may be a major oncogenic driver gene in BSARCC. The main interest in analyzing the *MET* status of tumors is that it may be of benefit for anti-*MET*-targeted therapies in the treatment of aggressive tumors. This may require the collection of more BSARCC cases to study their correlation.

In conclusion, the differential diagnosis of BSARCC is generally not difficult as long as its unique histological and immunophenotypic features can be recognized. BSARCC may have certain imaging manifestations similar to those of PRCC, but BSARCC primarily occurs in the renal medulla, which may be one of its comparative features on imaging. In the future, we expect to collect more imaging data to improve our understanding of BSARCC.

Acknowledgments

Funding: None.

Footnote

Conflicts of Interest: All authors have completed the ICMJE uniform disclosure form (available at https://qims.amegroups.com/article/view/10.21037/qims-21-1230/coif). The authors have no conflicts of interest to declare.

Ethical Statement: The authors are accountable for all aspects of the work in ensuring that questions related to the accuracy or integrity of any part of the work are appropriately investigated and resolved. All procedures performed in this study were in accordance with the ethical standards of the institutional and/or national research committee(s) and with the Helsinki Declaration (as revised in 2013). Written informed consent was obtained from the patient or legal guardian for publication of this case report and accompanying images. A copy of the written consent is available for review by the editorial office of this journal.

References

1. Petersson F, Bulimbasic S, Hes O, Slavik P, Martínek P, Michal M, Gomolčáková B, Hora M, Damjanov I. Biphasic alveolosquamoid renal carcinoma: a histomorphological, immunohistochemical, molecular genetic, and ultrastructural study of a distinctive morphologic variant of renal cell carcinoma. Ann Diagn Pathol 2012;16:459-69.
2. Hes O, Condom Mundo E, Peckova K, Lopez JI, Martinek P, Vanecek T, et al. Biphasic Squamoid Alveolar Renal Cell Carcinoma: A Distinctive Subtype of Papillary Renal Cell Carcinoma? Am J Surg Pathol 2016;40:664-75.
3. Trpkov K, Athanazio D, Magi-Galluzzi C, Yilmaz H, Clouston D, Agaimy A, Williamson SR, Brimo F, Lopez JI, Ulamec M, Rioux-Leclercq N, Kassem M,

Gupta N, Hartmann A, Leroy X, Bashir SA, Yilmaz A, Hes O. Biphasic papillary renal cell carcinoma is a rare morphological variant with frequent multifocality: a study of 28 cases. Histopathology 2018;72:777-85.
4. Delahunt B, Eble JN, Egevad L, Yaxley J, Thunders M, Samaratunga H. Emerging entities of renal cell neoplasia. Surg Exp Pathol 2019;2:10.
5. Moch H, Cubilla AL, Humphrey PA, Reuter VE, Ulbright TM. The 2016 WHO Classification of Tumours of the Urinary System and Male Genital Organs-Part A: Renal, Penile, and Testicular Tumours. Eur Urol 2016;70:93-105.
6. Trpkov K, Hes O. New and emerging renal entities: a perspective post-WHO 2016 classification. Histopathology 2019;74:31-59.
7. Troxell ML, Higgins JP. Renal cell carcinoma in kidney allografts: histologic types, including biphasic papillary carcinoma. Hum Pathol 2016;57:28-36.
8. Lopez JI. Case Report: Multifocal biphasic squamoid alveolar renal cell carcinoma. F1000Res 2016;5:607.
9. Chartier S, Méjean A, Richard S, Thiounn N, Vasiliu V, Verkarre V. Biphasic Squamoid Alveolar Renal Cell Carcinoma: 2 Cases in a Family Supporting a Continuous Spectrum With Papillary Type I Renal Cell Carcinoma. Am J Surg Pathol 2017;41:1011-2.
10. Zhou L, Xu H, Zhou Y, Zhou J, Zhang P, Yang X, Wang C. Biphasic squamoid alveolar renal carcinoma with positive CD57 expression: A clinicopathologic study of three cases. Pathol Int 2019;69:519-25.
11. Denize T, Just PA, Sibony M, Blons H, Timsit MO, Drossart T, Jakubowicz D, Broudin C, Morini A, Molina T, Vano Y, Auvray-Kuentz M, Richard S, Mejean A, Gimenez Roqueplo AP, Burnichon N, Verkarre V. MET alterations in biphasic squamoid alveolar papillary renal cell carcinomas and clinicopathological features. Mod Pathol 2021;34:647-59.
12. Sun MR, Ngo L, Genega EM, Atkins MB, Finn ME, Rofsky NM, Pedrosa I. Renal cell carcinoma: dynamic contrast-enhanced MR imaging for differentiation of tumor subtypes--correlation with pathologic findings. Radiology 2009;250:793-802.
13. Roy C, Sauer B, Lindner V, Lang H, Saussine C, Jacqmin D. MR Imaging of papillary renal neoplasms: potential application for characterization of small renal masses. Eur Radiol 2007;17:193-200.
14. Tsuda K, Kinouchi T, Tanikawa G, Yasuhara Y, Yanagawa M, Kakimoto K, Ono Y, Meguro N, Maeda O, Arisawa J, Usami M. Imaging characteristics of papillary renal cell carcinoma by computed tomography scan and magnetic resonance imaging. Int J Urol 2005;12:795-800.
15. Namura K, Minamimoto R, Yao M, Makiyama K, Murakami T, Sano F, Hayashi N, Tateishi U, Ishigaki H, Kishida T, Miura T, Kobayashi K, Noguchi S, Inoue T, Kubota Y, Nakaigawa N. Impact of maximum standardized uptake value (SUVmax) evaluated by 18-Fluoro-2-deoxy-D-glucose positron emission tomography/computed tomography (18F-FDG-PET/CT) on survival for patients with advanced renal cell carcinoma: a preliminary report. BMC Cancer 2010;10:667.
16. Pal SK, Ali SM, Yakirevich E, Geynisman DM, Karam JA, Elvin JA, Frampton GM, Huang X, Lin DI, Rosenzweig M, Lipson D, Stephens PJ, Ross JS, Miller VA, Agarwal N, Shuch B, Choueiri TK, Chung JH. Characterization of Clinical Cases of Advanced Papillary Renal Cell Carcinoma via Comprehensive Genomic Profiling. Eur Urol 2018;73:71-8.

Cite this article as: Zhang Y, Xu Y, Yu T, Chen J, Zhao M, Lin C. Biphasic squamoid alveolar renal cell carcinoma: description of a rare case and a literature analysis. Quant Imaging Med Surg 2022;12(7):3987-3994. doi: 10.21037/qims-21-1230

